Biochemical and Biophysical Research Communications 461 (2015) 575–581

Contents lists available at ScienceDirect

Biochemical and Biophysical Research Communications

journal homepage: www.elsevier.com/locate/ybbrc

Necroptosis mediated by *receptor* interaction protein kinase 1 and 3 aggravates chronic kidney injury of subtotal nephrectomised rats

Yongjun Zhu [a], Hongwang Cui [b], Hua Gan [a, *], Yunfeng Xia [a, *], Lizhen Wang [c], Yuxuan Wang [a], Yue Sun [a]

[a] Department of Nephrology, The First Affiliated Hospital of Chongqing Medical University, Chongqing, China
[b] Department of Orthopaedics, The First Affiliated Hospital of Chongqing Medical University, Chongqing, China
[c] Department of Pathology, Wannan Medical College, Wuhu, China

ARTICLE INFO

Article history:
Received 25 March 2015
Available online 20 April 2015

Keywords:
Necroptosis
RIP1
RIP3
Chronic kidney disease

ABSTRACT

Necroptosis, an alternative mode of programmed cell death, has crucial pathophysiological roles in many diseases, but its effect on chronic kidney disease (CKD) is poorly understood. Therefore, we assessed necroptosis and its pathophysiological effects in a widely used remnant-kidney rat model. *We* found that necroptotic cell death and the highest level of receptor interaction protein kinase 1 (RIP1) and receptor interaction protein kinase 3 (RIP3), critical signalling molecules for necroptosis, appeared 8 weeks after subtotal nephrectomy (SNX) surgery. After treatment with Necrostatin-1 (Nec-1), renal function and renal pathologic changes were significantly improved; the overexpression of RIP1, RIP3, mixed lineage kinase domain-like (MLKL) and dynamin-related protein 1 (Drp1) was reduced; and necroptosis was inhibited. These results indicated that necroptosis mediated by RIP1 and RIP3 participates in the loss of renal cells of subtotal nephrectomised rats and might be one of main causes of the excessive loss of renal cells during the sustained progression of renal fibrosis.

1. Introduction

The pathological changes of chronic kidney disease (CKD) begin with the excessive loss of critical nephrons, which is followed by progressive glomerular sclerosis, the collapse of peritubular capillaries and tubular interstitial fibrosis. *Whatever the nature of the* insult, even if the initial lesion has healed or improved, the remaining nephrons continue to be lost and renal fibrosis lesions progress until end-stage renal failure has occurred. Therefore, exploring the mechanism of the progressive loss of nephrons and blocking this process are widely believed to be effective ways to prevent the progression of CKD.

Necrosis is believed to occur as an accident or unregulated event. However, recent studies showed that some types of cell necrosis share similar features with programmed cell death, which can be regulated [1,2]. *This type of* cell death mode is named as necroptosis [3].

Necroptosis is a caspase-independent programmed cell death that is mediated by death receptors and regulated by accurate cell signal pathways [3]. In the necroptosis pathways, receptor interaction protein kinase 1 and 3 (RIP1/3) play a vital role [4–6]. In response to upstream signal molecules, RIP1 undergoes a series of ubiquitination, deubiquitination and phosphorylation events. When caspase-8 is inhibited, the activated RIP1 triggers the phosphorylation of RIP3 kinases and forms the necrosome, which can drive necroptosis [7]. Necrostatin-1 (Nec-1, a specific inhibitor of RIP1) can inhibit RIP1 kinase activity and stop necroptosis [8].

Recent studies found that necroptosis is the main form of tubular cell loss in acute ischemia/reperfusion renal injury [9]. However, the role of necroptosis in the progression of CKD is still unknown. Therefore, we sought to *test* the hypothesis that necroptosis is an important form of renal cell death during the

Abbreviations: CKD, chronic kidney disease; RIP1, receptor interaction protein kinase 1; RIP3, receptor interaction protein kinase 3; SNX, subtotal nephrectomy; Nec-1, Necrostatin-1; MLKL, mixed lineage kinase domain-like; PGAM5, phosphoglycerate mutase family member 5; Drp1, dynamin-related protein 1; ROS, reactive oxygen species; GSI, glomerular sclerosis index; TIS, tubulointerstitial damage scores; DAPI, 4′, 6-diamidino-2-phenylindole; RHIM, RIP homotypic interaction motif; TNFR1, tumor necrosis factor receptor1; qPCR, *quantitative* real-time PCR.

* Corresponding authors. Department of Nephrology, The First Affiliated Hospital of Chongqing Medical University, Youyi Road 1, Chongqing 400016, China. Fax: +86 236881148.
E-mail addresses: cqchw2013@sina.com (H. Gan), xyf09200@126.com (Y. Xia).

http://dx.doi.org/10.1016/j.bbrc.2015.03.164
0006-291X/

progression of CKD and *is* mediated by RIP1 and RIP3 signalling pathways.

2. Materials and methods

2.1. Animals

Eight-week-old healthy male Sprague–Dawley (250 g–300 g in body weight) rats used in this study were supplied by the *Animal Laboratory Centre* of Chongqing Medical University. All rats were housed under standard conditions with a 12-h light–dark cycle, given free access to water and fed a standard rodent diet. All animal experimental protocols were performed in strict accordance with standards stated in the NIH Guidelines for the Care and Use of Laboratory Animals and were approved by the biomedical research ethics committee of Chongqing Medical University.

2.2. Establishment of the subtotal nephrectomised rat model

After a 7-day adaptation period, Sprague–Dawley (SD) rats were randomly assigned to the subtotal nephrectomy (SNX) group (n = 54) or control group (n = 36). SD rats were subjected to subtotal nephrectomy surgery in the SNX group and sham surgery in the control group as reported previously [10,11]. Briefly, the right kidneys of rats in the SNX group were removed under intraperitoneal anaesthesia with pentobarbital sodium. Seven days later, the upper and lower cortex of the left kidney (approximately 60%–70% of the right kidney *by weight*) was removed, and 1/3 of the left kidney was *preserved*. Rats in the control group underwent renal decapsulation *only*.

2.3. Drug administration

Z-VAD-fmk (Z-VAD, MP Biomedicals, Solon, OH, USA) and Necrostatin-1 (Nec-1, Sigma–Aldrich, *St. Louis., MO, USA*) were dissolved in 10% dimethyl sulfoxide (DMSO, Sigma, USA). Rats underwent the SNX surgery, recovered for 4 weeks, were injected intraperitoneally with Z-VAD (1.0 mg/kg/d [12]) or Nec-1 (1.65 mg/kg/d [9]) or an equal volume of 10% DOSM (vehicle) and were maintained for 4 more weeks. At 8 weeks after surgery, the rats were sacrificed.

2.4. Renal function

Serum urea nitrogen and creatinine concentrations were used to assess renal function and *were* assayed using an automatic biochemical analyser (Roche Hx-49, Mannheim, Germany).

2.5. Renal morphology

The remnant kidney tissue was fixed in 10% formalin buffer and embedded in paraffin. Four-micrometre-thick sections of the kidney were stained with periodic acid–Schiff (PAS) for morphological analysis in a double-blind fashion to determine the extent of renal injury. The glomerular sclerosis index (GSI) and the *tubulointerstitial* damage scores (TIS) *were* assessed [13,14].

2.6. Transmission electron microscopy (TEM)

Several pieces of 1-mm^3 renal tissue fragments were fixed in 2.5% glutaraldehyde phosphate buffer (pH 7.4) overnight at 4 °C. Then, the tissue fragments were fixed in 2% osmium tetroxide for 1 h and block-stained with 2% uranyl acetate. Next, the kidney tissues were embedded in epoxy resin and dehydrated. Then, ultrathin sections were used and stained with uranyl acetate and subsequently stained with lead citrate. The ultrastructure of kidney tissues was observed by electron microscopy (Hitachi-7500, Japan).

2.7. Quantitative real-time PCR (qPCR)

Total RNA was extracted from kidney tissue with RNAiso Plus (Total RNA extraction reagent, TaKaRa BIO INC. Japan). Approximately 1000 ng of total RNA was reverse transcribed with the Prime Script® ™ RT Reagent Kit with gDNA Erase (TaKaRa BIO INC. Japan) and amplified in triplicate using SYBR® Premix Ex TaqTM II (TaKaRa BIO INC. Japan) with a CFX96TM Real-Time PCR detection system (Bio-Rad, California, USA), according to the manufacturer's instructions. The following primer sequences were used (forward and reverse): RIP1, forward 5′-AGGTACAGGAGTTTGGTATGGGC-3′ and reverse 5′-GGTGGTGCCAAGGAG ATGTATG-3'; RIP3, forward 5′-TAGTTTATGAAATGCTGGACCGC-3′ and reverse 5′-GCCAAGGTGTCAGATGATGTCC-3'. Gene expression relative to the housekeeping gene GAPDH was determined using the $2^{-\Delta\Delta Ct}$ method.

2.8. Western blotting

Kidney tissue was lysed with RIPA lysate buffer (Beyotime, Jiangsu, China), and the protein concentration was determined using a BCA protein quantitative kit (Beyotime, Jiangsu, China). Equal amounts of protein were separated on a SDS-PAGE gel, and the proteins were transferred to a PVDF membrane (EMD Millipore, USA). Immunoblotting was performed according to standard procedures with the following primary antibodies: anti-RIP1 monoclonal antibody (R&D Systems, Minneapolis, MN, USA), anti-RIP3 polyclonal antibody (Abcam Inc., Cambridge, USA), anti-PGAM5 polyclonal antibody and anti-MLKL polyclonal antibody (Santa Cruz Biotechnology, California, USA), anti-Drp1 polyclonal antibody (Cell Signalling Technology, Boston, USA), and anti-β-actin monoclonal antibody (Santa Cruz Biotechnology, California, USA). Western *blotting* was performed using conventional methods as described previously [15].

2.9. Immunofluorescence staining

Kidney paraffin sections (4 μm) were deparaffinised and incubated with a mouse anti-RIP1 antibody (R&D Systems, Minneapolis, MN, USA) and rabbit anti-RIP3 antibody (Abcam Inc., Cambridge, USA). The secondary antibodies were Alexa *Fluor* 488-labelled goat anti-mouse *and* Cy3-labelled donkey anti-rabbit (Beyotime, Jiangsu, China). The sections were counterstained with mounting medium containing DAPI. Confocal images were acquired using *laser* confocal microscopy (Leica TCP SP5, Leica Microsystems GmbH, Wetzlar, Germany).

2.10. Reactive oxygen species (ROS) level

The ROS level in kidney tissue was tested as previously described [16]. Briefly, the kidney tissue was homogenised with ice-cold PBS buffer to obtain a concentration of 5 mg tissue/ml and centrifuged to collect the supernatant. Then, the fluorescence probe DCFH-DA (NanJing JianCheng Bioengineering, Nanjing, China) was added to the supernatant, and the two were incubated together at 37 °C for 30 min. The fluorescence intensity of the DCF product was measured using a spectrofluorimeter with excitation at 484 nm and emission at 530 nm. Parts of the homogenate supernatant were used to test the protein concentration with a BCA protein quantitative kit (Beyotime, Jiangsu, China). Fluorescence intensity/protein concentration was calculated.

2.11. Statistical analysis

All data were expressed as *mean* ± SEM. The SPSS 17.0 statistical software program (SPSS Inc., IL, USA) was used for statistical analyses. Multiple group comparisons were performed by one-way ANOVA followed by the Bonferroni procedure for comparison of means. $P < 0.05$ was considered statistically significant.

3. Results

3.1. The induction of necroptosis in the rat remnant kidney after subtotal nephrectomy (SNX) surgery

In the remnant kidney of vehicle-treated rats, expansion *of the* renal tubular cell volume, swelling of the organelles, rupture of the plasma membrane, loss of cell organelle contents and extensive formation of intracellular vacuoles were found 8 weeks after surgery by TEM (Fig. 1A). *These findings* were consistent with the typical morphological features of necroptotic cell death [7,9]. However, obvious necrotic changes in the renal cells were not found at 4 *or* 12 weeks after surgery (Fig. 1A). The qPCR analysis demonstrated that RIP1 and RIP3 mRNA expression in the remnant kidney increased notably by 4 weeks after SNX surgery and attained the peak elevation by 8 weeks. *Subsequently,* a sharp decrease was found by 12 weeks (Fig. 1B). Western blot analyses also revealed that both RIP1 and RIP3 *proteins* in the rat remnant kidney attained peak expression at 8 weeks (Fig. 1C). These data indicated that the highest peak of necroptosis in the rat remnant kidney occurred 8 weeks after SNX surgery.

3.2. Inhibition of necroptosis by Nec-1 can alleviate kidney injury of subtotal nephrectomised rats

Obvious glomerulosclerosis and tubulointerstitial fibrosis *were* found on PAS-stained paraffin sections; *in particular,* the tubular and interstitial lesions were quite *substantial* (Fig. 2A). The glomerular sclerosis index and tubulointerstitial damage scores were dramatically higher than those of the control group (Fig. 2B, C). Treatment with Nec-1 substantially reduced the glomerular damage and tubular and interstitial lesions (Fig. 2B, C).

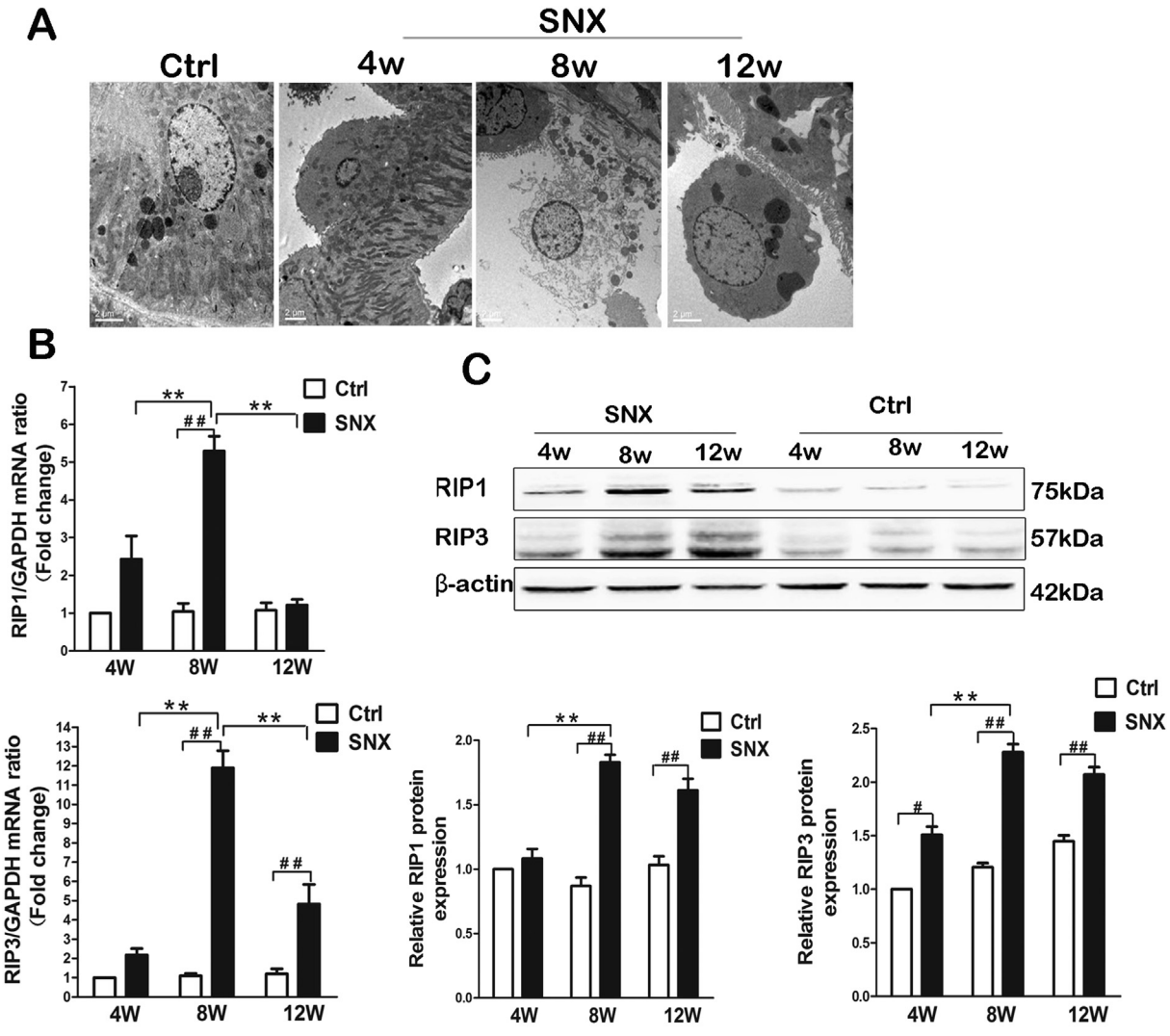

Fig. 1. Induction of necroptosis in the remnant kidney of subtotal nephrectomised rats at various time points. (A) *Necroptotic* cells with typical necrotic morphological features were observed in the rat remnant kidney after SNX surgery by TEM. Scale bar represents 2 μm. (B) Quantitative real-time PCR analysis for RIP1 *and* RIP3 mRNA expression in the rat remnant kidney at 4, 8, and 12 weeks after SNX surgery, n = 8 per group. (C) Western blot analysis for RIP1 *and* RIP3 protein expression in the rat remnant kidney at 4, 8, and 12 weeks after SNX surgery, n = 8 per group. $^{\#}p < 0.05$, $^{\#\#}p < 0.01$ versus control group; $^{*}p < 0.05$, $^{**}p < 0.01$ versus SNX 8W group. Ctrl indicates control. SNX indicates subtotal nephrectomy.

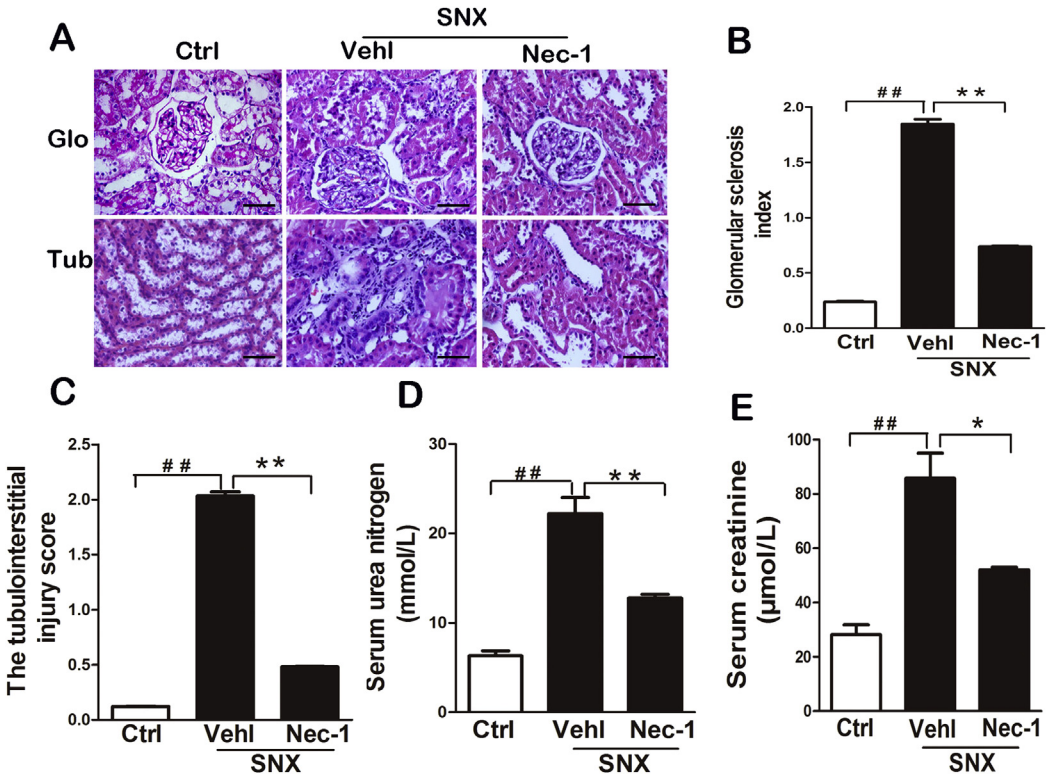

Fig. 2. Effect of Nec-1 on renal morphology and renal function of subtotal nephrectomised rats. (A) Representative photomicrographs of PAS-stained sections showing kidney injury in glomerular and tubulointerstitial compartments of subtotal nephrectomised rats 4 weeks after Nec-1 or vehicle treatment. Scale bar represents 25 μm. (B, C) Quantitative analysis of the glomerular sclerosis index (GSI) and the tubulointerstitial damage scores (TIS) of subtotal nephrectomised rats 4 weeks after Nec-1 or vehicle treatment, n = 6 per group. (D, E) Nec-1 significantly attenuated renal dysfunction of subtotal nephrectomised rats 4 weeks after Nec-1 or vehicle treatment. n = 6 per group. $^{\#}p < 0.05$, $^{\#\#}p < 0.01$ versus the control group; $^{*}p < 0.05$, $^{**}p < 0.01$ versus the SNX + vehicle group. Ctrl indicates control, SNX indicates subtotal nephrectomy, Vehl indicates vehicle, Glo indicates glomeruli, Tub indicates tubulointerstitium.

Furthermore, we found that treatment with Nec-1 reduced the increased concentration of urea nitrogen and creatinine of subtotal nephrectomised rats (Fig. 2D, E).

3.3. *Nec-1 inhibits the expression of RIP1 and RIP3 in the rat remnant kidney*

We studied the localisation of RIP1 and RIP3 in remnant kidney cells by immunofluorescence analyses. By confocal microscopy, we observed that RIP1 colocalised abundantly with RIP3 in tubular cells of the remnant kidney, especially in the cytoplasm of proximal tubular epithelial cells. *However,* the proteins were not detected, or only scarcely detected, in glomeruli (Fig. 3A).

The qPCR analysis showed that Nec-1 significantly *inhibited* the elevated expression of RIP1 and RIP3 mRNA in the remnant kidney; however, Z-VAD did not reduce RIP1 and RIP3 mRNA levels (Fig. 3B). The western blot analysis showed consistent results with the expression of RIP1 and RIP3 mRNA previously described. Nec-1 notably *inhibited* the higher levels of RIP1 and RIP3 proteins in the remnant kidney, but Z-VAD had no effect (Fig. 3C).

3.4. *Necroptosis mediated by RIP1 and RIP3 in the rat remnant kidney is executed via the MLKL, Drp1, and ROS signalling molecules*

We found that MLKL protein expression in the remnant kidney was significantly higher than in the control group. After treatment with Nec-1, MLKL overexpression was reduced, but Z-VAD had no role (Fig. 4A). These results were consistent with the changes observed in the RIP1 and RIP3 proteins.

Furthermore, western blot analysis indicated that the protein expression of PGAM5 and Drp1 was elevated in the rat remnant kidney compared with that of the control group. No notable decrease of PGAM5 was found in Z-VAD-treated and Nec-1 treated subtotal nephrectomised rats (Fig. 4B). However, Z-VAD and Nec-1 significantly reduced Drp1 protein overexpression in the remnant kidney (Fig. 4B).

In addition, the results showed elevated ROS levels in the rat remnant kidney tissue and a noticeable reduction in these levels after Z-VAD and Nec-1 treatment (Fig. 4C).

4. Discussion

In some studies, scientists have found that apoptosis might be the primary cause of renal cell death of subtotal nephrectomised rats [17,18]. Unfortunately, this study indicated that inhibition of apoptosis by Z-VAD, a pan-caspase inhibitor, could not effectively reduce the increased number of TUNEL-positive cells in the remnant kidney of subtotal nephrectomised rats (Figure S). This result suggested that the excessive loss of remnant kidney cells was caused by other forms of cell death, such as necroptosis. In this study, necroptotic cells with typical morphological features were observed by TEM in the rat remnant kidney 8 weeks after surgery. We also found that the expression of RIP1 and RIP3, critical signalling molecules for necroptosis, attained peak expression 8 weeks after surgery. These results indicated that necroptosis, an alternative cell death pathway, participated in the excessive loss of cells in the remnant kidney during the sustained progression of renal fibrosis.

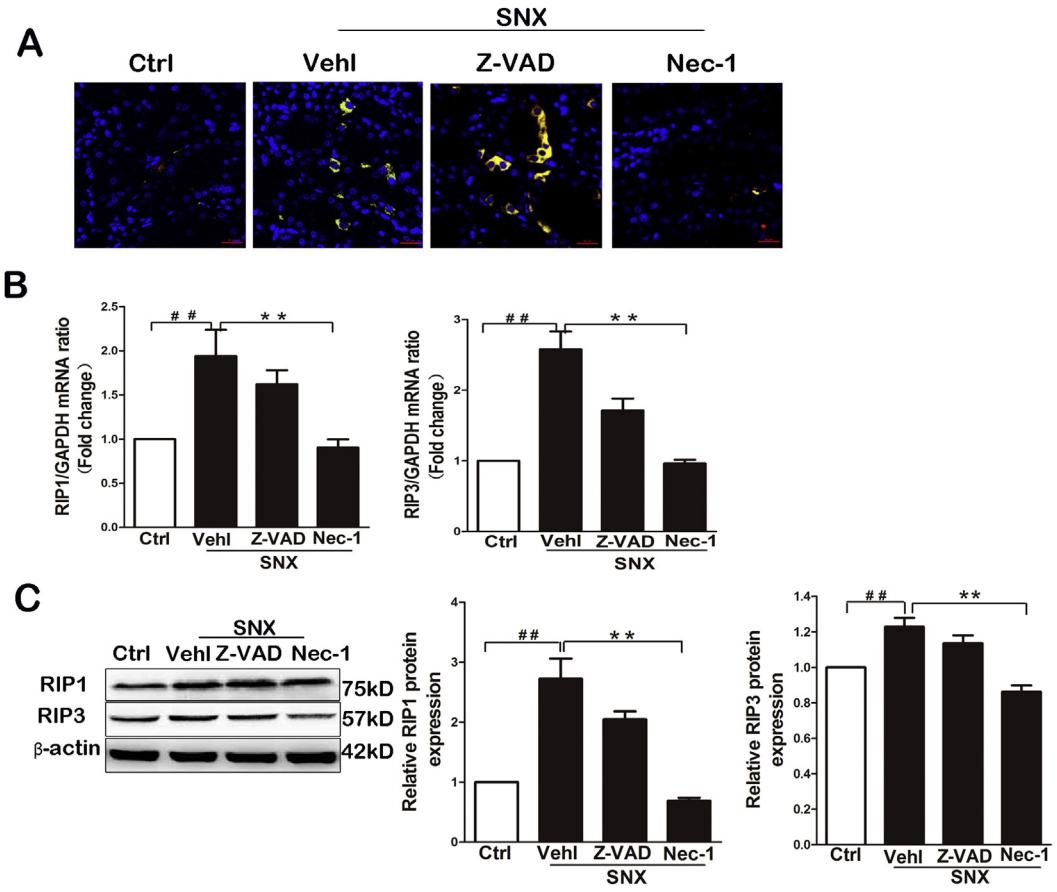

Fig. 3. Effect of Nec-1 on RIP1 and RIP3 expression in the rat remnant kidney. (A) Representative photomicrographs of kidney sections from subtotal nephrectomised rats 4 weeks after Z-VAD or Nec-1 or vehicle treatment stained for RIP1 (green), RIP3 (red), and DAPI (4′, 6-diamidino-2-phenylindole, blue). RIP1 and RIP3 double positive cells *are indicated in* yellow. Scale bar represents 20 μm. (B) Quantitative real-time PCR analysis for RIP1 *and* RIP3 mRNA expression in the remnant kidney of subtotal nephrectomised rats 4 weeks after Z-VAD or Nec-1 or vehicle treatment, n = 6 per group. (C) Western blot analysis for RIP1 *and* RIP3 protein expression in the remnant kidney of subtotal nephrectomised rats 4 weeks after Z-VAD or Nec-1 or vehicle treatment, n = 6 per group. $^{\#}p < 0.05$, $^{\#\#}p < 0.01$ versus the control group; $^{*}p < 0.05$, $^{**}p < 0.01$ versus the SNX + vehicle group. Ctrl indicates control, SNX indicates subtotal nephrectomy, Vehl indicates vehicle. (For interpretation of the references to colour in this figure legend, the reader is referred to the web version of this article.)

Necroptosis is a cell death receptor-induced, caspase-independent, highly regulated programmed process of cell death with morphological resemblance to necrosis [19]. The most important feature of necroptosis is that it can be specifically inhibited by a small molecule, Nec-1, which targets the death domain of the RIP1 kinase but cannot be blocked by an inhibitor of apoptosis, such as Z-VAD [20]. In this experiment, we found that Nec-1 treatment significantly reduced RIP1and RIP3 overexpression in the remnant kidney, but the increased expression could not be suppressed by Z-VAD. This result agreed with the above features of necroptosis and further confirmed that necroptosis is involved in cell death in the rat remnant kidney.

RIP1 and RIP3 are members of the receptor interacting protein family, and their kinase activity plays a critical role in necroptosis [6,8,21]. RIP1 is a pleiotropic adaptor that is associated with death receptors, such as Fas and TNFR1. When a death receptor is triggered, RIP1 is recruited to the signalling complex of death receptors and is polyubiquitinated [19,22]. Following deubiquitination, activated RIP1 and RIP3 form the necrosome and initiate necroptosis when the apoptotic pathway is inhibited [22]. RIP3, an essential component of death receptor-induced programmed necrosis, is a determinant factor for necroptosis. RIP1 and RIP3 form a intracytoplasmic RIP1-RIP3 complex during programmed necrosis, which is called necrosome-mediated necroptotic cell death [23]. Consistent with these studies, we found that the expression of RIP1 and RIP3, critical signalling molecules of necroptosis, was much higher than that in the control group 8 weeks after SNX surgery. Simultaneously, we observed that RIP1 colocalised prominently with RIP3 in tubular epithelial cells in the remnant kidney. These findings indicated that necroptosis in the rat remnant kidney was mediated by both RIP1and RIP3.

New studies have found that MLKL, a key downstream signal molecule of RIP3, can form the RIP1-RIP3-MLKL complex with RIP1 and RIP3 to trigger necroptosis [24]. PGAM5, another substrate of RIP3 [25], and Drp1 can form the mitochondrial attack complex to induce ROS overproduction and necroptosis [25]. Drp1, a member of the dynamin family of GTPases [26], facilitates mitochondrial division [27] and contributes to cell death [28]. However, the roles of PGAM5 and Drp1 in necroptosis are highly controversial, as various papers have demonstrated them not to be required for necroptosis [29]. In this study, we found that the expression of MLKL and Drp1 in the remnant kidney was increased, and Nec-1 *attenuated these* expression levels. These results were roughly consistent with the changes in RIP1 and RIP3 expression and indicated that MLKL and Drp1, downstream signalling molecules of RIP1 and RIP3, participated in signalling pathways promoting remnant renal cell necroptosis. However, we also found that Nec-1 did not decrease the increased expression of PGAM5 protein in the

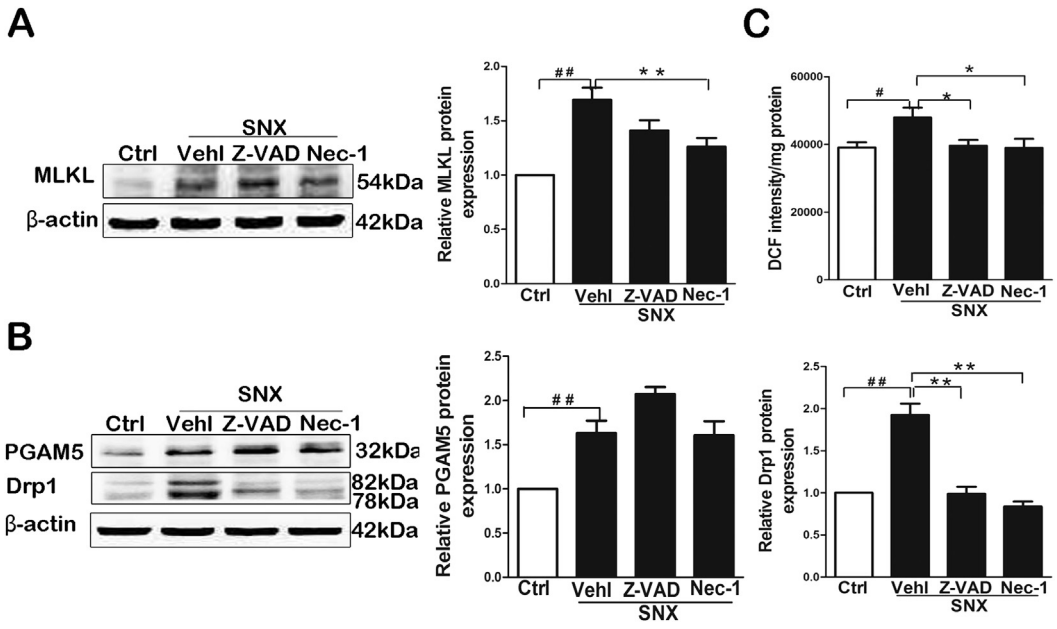

Fig. 4. Effect of Nec-1 on the expression of MLKL, PGAM5, Drp1 and ROS in the rat remnant kidney. (A) Western blot analysis for MLKL protein expression in the remnant kidney of subtotal nephrectomised rats 4 weeks after Z-VAD or Nec-1 or vehicle treatment, n = 6 per group. (B) Western blot analysis for PGAM5 *and* Drp1 protein expression in the remnant kidney of subtotal nephrectomised rats 4 weeks after Z-VAD or Nec-1 or vehicle treatment, n = 6 per group. (C) DCFH-DA analysis for the ROS level in the remnant kidney of subtotal nephrectomised rats 4 weeks after Z-VAD or Nec-1 or vehicle treatment, n = 6 per group. $^{\#}p < 0.05$, $^{\#\#}p < 0.01$ versus the control group; $^{*}p < 0.05$, $^{**}p < 0.01$ versus the SNX + vehicle group. Ctrl indicates control, SNX indicates subtotal nephrectomy, Vehl indicates vehicle.

remnant kidney. The results indicated that PGAM5 might not be required for necroptosis of remnant renal cells, which was consistent with the above opinion from Tait et al. [26].

The overproduction of reactive oxygen species (ROS) plays the critical role in the execution of necroptosis [25,30]. RIP1 and RIP3 act as upstream signalling molecules to regulate ROS production during programmed necrosis by engaging the mitochondrial metabolism machinery [8,23,31]. Consistent with this conclusion, we found that ROS were overproduced in the remnant kidney tissue of subtotal nephrectomised rats, and the accumulated ROS could be controlled by Nec-1 treatment. These data further indicated that ROS, the downstream signalling molecule of RIP1 and RIP3, might be the executioner of necroptotic cell death in the remnant kidney.

With the sustained and slow progression of CKD, progressive renal cell loss is frequently followed by the persistent deterioration of kidney function and renal fibrosis. However, current therapies cannot prevent *this* malignant progression in a considerable proportion of CKD patients. Therefore, it is necessary to develop effective drugs with therapeutic value. In this study, we confirmed that necroptosis mediated by RIP1 and RIP3 might be an important mode of renal cell death during the progression of CKD, and its specific inhibitors, such as Nec-1, could suppress necroptosis by interrupting *the* RIP1/RIP3 signalling pathway. *Therefore, we identified* Nec-1 as a novel therapeutic strategy for delaying the progression of CKD.

Competing financial interests

The authors declare no competing financial interests.

Conflict of interest

The authors declare that there are no conflicts of interest.

Acknowledgments

This study was funded by the Chinese National Science and Technology Support Plan (2011BAI10B01).

Appendix A. Supplementary data

Supplementary data related to this article can be found at http://dx.doi.org/10.1016/j.bbrc.2015.03.164.

Transparency document

Transparency document related to this article can be found online at http://dx.doi.org/10.1016/j.bbrc.2015.03.164.

References

[1] G. Kroemer, L. Galluzzi, P. Vandenabeele, J. Abrams, E.S. Alnemri, E.H. Baehrecke, M.V. Blagosklonny, W.S. El-Deiry, P. Golstein, D.R. Green, M. Hengartner, R.A. Knight, S. Kumar, S.A. Lipton, W. Malorni, G. Nunez, M.E. Peter, J. Tschopp, J. Yuan, M. Piacentini, B. Zhivotovsky, G. Melino, Classification of cell death: recommendations of the nomenclature Committee on cell deatxzh 2009, Cell. Death Differ. 16 (2009) 3–11.
[2] I.L. Ch'en, J.S. Tsau, J.D. Molkentin, M. Komatsu, S.M. Hedrick, Mechanisms of necroptosis in T cells, J. Exp. Med. 208 (2011) 633–641.
[3] A. Degterev, Z. Huang, M. Boyce, Y. Li, P. Jagtap, N. Mizushima, G.D. Cuny, T.J. Mitchison, M.A. Moskowitz, J. Yuan, Chemical inhibitor of nonapoptotic cell death with therapeutic potential for ischemic brain injury, Nat. Chem. Biol. 1 (2005) 112–119.
[4] W. Wu, P. Liu, J. Li, Necroptosis: an emerging form of programmed cell death, Crit. Rev. Oncol. Hematol. 82 (2012) 249–258.
[5] D.W. Zhang, J. Shao, J. Lin, N. Zhang, B.J. Lu, S.C. Lin, M.Q. Dong, J. Han, RIP3, an energy metabolism regulator that switches TNF-induced cell death from apoptosis to necrosis, Science 325 (2009) 332–336.
[6] Y.S. Cho, S. Challa, D. Moquin, R. Genga, T.D. Ray, M. Guildford, F.K. Chan, Phosphorylation-driven assembly of the RIP1-RIP3 complex regulates programmed necrosis and virus-induced inflammation, Cell 137 (2009) 1112–1123.
[7] A. Linkermann, D.R. Green, Necroptosis, N. Engl. J. Med. 370 (2014) 455–465.
[8] D.E. Christofferson, J. Yuan, Necroptosis as an alternative form of programmed cell death, Curr. Opin. Cell. Biol. 22 (2010) 263–268.

[9] A. Linkermann, J.H. Brasen, N. Himmerkus, S. Liu, T.B. Huber, U. Kunzendorf, S. Krautwald, Rip1 (receptor-interacting protein kinase 1) mediates necroptosis and contributes to renal ischemia/reperfusion injury, Kidney Int. 81 (2012) 751–761.
[10] K. Amann, C. Nichols, J. Tornig, U. Schwarz, M. Zeier, G. Mall, E. Ritz, Effect of ramipril, nifedipine, and moxonidine on glomerular morphology and podocyte structure in experimental renal failure, Nephrol. Dial. Transpl. 11 (1996) 1003–1011.
[11] G. Piecha, G. Kokeny, K. Nakagawa, N. Koleganova, A. Geldyyev, I. Berger, E. Ritz, C.P. Schmitt, M.L. Gross, Calcimimetic R-568 or calcitriol: equally beneficial on progression of renal damage in subtotally nephrectomized rats, Am. J. Physiol. Ren. Physiol. 294 (2008) F748–F757.
[12] M. Baumann, B.J. Janssen, J.J. Rob Hermans, R. Bartholome, J.F. Smits, H.A. Struijker Boudier, Renal medullary effects of transient prehypertensive treatment in young spontaneously hypertensive rats, Acta Physiol. (Oxf) 196 (2009) 231–237.
[13] L. Raij, S. Azar, W. Keane, Mesangial immune injury, hypertension, and progressive glomerular damage in Dahl rats, Kidney Int. 26 (1984) 137–143.
[14] Z. Zhang, L. Sun, Y. Wang, G. Ning, A.W. Minto, J. Kong, R.J. Quigg, Y.C. Li, Renoprotective role of the vitamin D receptor in diabetic nephropathy, Kidney Int. 73 (2008) 163–171.
[15] Y. Tanaka, S. Kume, S. Araki, K. Isshiki, M. Chin-Kanasaki, M. Sakaguchi, T. Sugimoto, D. Koya, M. Haneda, A. Kashiwagi, H. Maegawa, T. Uzu, Fenofibrate, a PPARalpha agonist, has renoprotective effects in mice by enhancing renal lipolysis, Kidney Int. 79 (2011) 871–882.
[16] G.K. Shinomol, Muralidhara, Differential induction of oxidative impairments in brain regions of male mice following subchronic consumption of Khesari dhal (Lathyrus sativus) and detoxified Khesari dhal, Neurotoxicology 28 (2007) 798–806.
[17] G.L. Thomas, B. Yang, B.E. Wagner, J. Savill, A.M. El Nahas, Cellular apoptosis and proliferation in experimental renal fibrosis, Nephrol. Dial. Transpl. 13 (1998) 2216–2226.
[18] C. Li, S.W. Lim, B.K. Sun, B.S. Choi, G.L. S, A. Cox, D. Kelly, Y.S. Kim, J. Kim, B.K. Bang, C.W. Yang, Expression of apoptosis-related factors in chronic cyclosporine nephrotoxicity after cyclosporine withdrawal, Acta Pharmacol. Sin. 25 (2004) 401–411.
[19] Z. Dunai, P.I. Bauer, R. Mihalik, Necroptosis: biochemical, physiological and pathological aspects, Pathol. Oncol. Res. 17 (2011) 791–800.
[20] W. Han, J. Xie, L. Li, Z. Liu, X. Hu, Necrostatin-1 reverts shikonin-induced necroptosis to apoptosis, Apoptosis 14 (2009) 674–686.
[21] S. He, L. Wang, L. Miao, T. Wang, F. Du, L. Zhao, X. Wang, Receptor interacting protein kinase-3 determines cellular necrotic response to TNF-alpha, Cell 137 (2009) 1100–1111.
[22] J. Zhang, H. Zhang, J. Li, S. Rosenberg, E.C. Zhang, X. Zhou, F. Qin, M. Farabaugh, RIP1-mediated regulation of lymphocyte survival and death responses, Immunol. Res. 51 (2011) 227–236.
[23] S. Challa, F.K. Chan, Going up in flames: necrotic cell injury and inflammatory diseases, Cell. Mol. Life Sci. 67 (2010) 3241–3253.
[24] L. Sun, H. Wang, Z. Wang, S. He, S. Chen, D. Liao, L. Wang, J. Yan, W. Liu, X. Lei, X. Wang, Mixed lineage kinase domain-like protein mediates necrosis signaling downstream of RIP3 kinase, Cell 148 (2012) 213–227.
[25] F.K. Chan, E.H. Baehrecke, RIP3 finds partners in crime, Cell 148 (2012) 17–18.
[26] E. Smirnova, L. Griparic, D.L. Shurland, A.M. van der Bliek, Dynamin-related protein Drp1 is required for mitochondrial division in mammalian cells, Mol. Biol. Cell. 12 (2001) 2245–2256.
[27] A. Tanaka, R.J. Youle, A chemical inhibitor of DRP1 uncouples mitochondrial fission and apoptosis, Mol. Cell. 29 (2008) 409–410.
[28] S. Frank, B. Gaume, E.S. Bergmann-Leitner, W.W. Leitner, E.G. Robert, F. Catez, C.L. Smith, R.J. Youle, The role of dynamin-related protein 1, a mediator of mitochondrial fission, in apoptosis, Dev. Cell. 1 (2001) 515–525.
[29] S.W. Tait, A. Oberst, G. Quarato, S. Milasta, M. Haller, R. Wang, M. Karvela, G. Ichim, N. Yatim, M.L. Albert, G. Kidd, R. Wakefield, S. Frase, S. Krautwald, A. Linkermann, D.R. Green, Widespread mitochondrial depletion via mitophagy does not compromise necroptosis, Cell. Rep. 5 (2013) 878–885.
[30] N. Festjens, M. Kalai, J. Smet, A. Meeus, R. Van Coster, X. Saelens, P. Vandenabeele, Butylated hydroxyanisole is more than a reactive oxygen species scavenger, Cell. Death Differ. 13 (2006) 166–169.
[31] V. Temkin, Q. Huang, H. Liu, H. Osada, R.M. Pope, Inhibition of ADP/ATP exchange in receptor-interacting protein-mediated necrosis, Mol. Cell. Biol. 26 (2006) 2215–2225.